Title

Adrenergic signaling promotes the expansion of cancer stem-like cells of malignant peripheral nerve sheath tumors

Author Names and Affiliations

Rongsheng Huang [a,#], Atsushi Fujimura [a,b,#,*], Eiji Nakata [c], Shota Takihira [c], Hirofumi Inoue [d], Soichiro Yoshikawa [a], Takeshi Hiyama [a], Toshifumi Ozaki [c], Atsunori Kamiya [a]

# These authors equally contributed to this work.

* Correspondence should be addressed to A. Fujimura: atsushi.fujimura@okayama-u.ac.jp

[a] Department of Cellular Physiology, Okayama University Graduate School of Medicine, Dentistry, and Pharmaceutical Sciences, 2-5-1 Shikata-cho, Kita-ku, Okayama 700-8558, Japan

[b] Neutron Therapy Research Center, Okayama University, 2-5-1 Shikata-cho, Kita-ku, Okayama 700-8558, Japan

[c] Department of Orthopedic Surgery, Okayama University Graduate School of Medicine,

Dentistry, and Pharmaceutical Sciences, 2-5-1 Shikata-cho, Kita-ku, Okayama 700-8558, Japan

[d] Department of Clinical Genetics and Genomic Medicine, Okayama University Graduate School of Medicine, Dentistry, and Pharmaceutical Sciences, 2-5-1 Shikata-cho, Kita-ku, Okayama 700-8558, Japan

Corresponding Author

Atsushi Fujimura, M.D., Ph.D.

Department of Cellular Physiology, Okayama University Graduate School of Medicine, Dentistry, and Pharmaceutical Sciences

2-5-1 Shikata-cho, Kita-ku, Okayama 700-8558, Japan

Tel: +81-86-235-7105

Fax: +81-86-235-7111

E-mail: atsushi.fujimura@okayama-u.ac.jp

Abstract

Malignant peripheral nerve sheath tumor (MPNST), a highly malignant tumor that arises in peripheral nerve tissues, is known to be highly resistant to radiation and chemotherapy. Although there are several reports on genetic mutations and epigenetic changes that define the pathogenesis of MPNST, there is insufficient information regarding the microenvironment that contributes to the malignancy of MPNST. In the present study, we demonstrate that adrenaline increases the cancer stem cell population in MPNST. This effect is mediated by adrenaline stimulation of beta-2 adrenergic receptor (ADRB2), which activates the Hippo transducer, YAP/TAZ. Inhibition and RNAi experiments revealed that inhibition of ADRB2 attenuated the adrenaline-triggered activity of YAP/TAZ and subsequently attenuated MPNST cells stemness. Furthermore, ADRB2-YAP/TAZ axis was confirmed in the MPNST patients' specimens. The prognosis of patients with high levels of ADRB2 was found to be significantly worse. These data show that adrenaline exacerbates MPNST prognosis and may aid the development of new treatment strategies for MPNST.

Keywords

MPNST

Cancer stem-like cells

ADRB2

YAP/TAZ

Abbreviations

MPNST, malignant peripheral nerve sheath tumor

ADRB2, beta-2 adrenergic receptor

NF1, neurofibromin 1

NGFR, nerve growth factor receptor

GSEA, Gene Set Enrichment Analysis

1. Introduction

Malignant peripheral nerve sheath tumor (MPNST) arises from malignant transformation of Schwann cells surrounding peripheral nerves [1]. Since the tumor cells extensively infiltrate along nerve branches, making complete surgical removal difficult, and are highly resistant to radiation and chemotherapy, recurrence and metastasis are

often observed in many cases and the 5-year survival rate remains low, even with multidisciplinary treatment [2–4].

Although many literatures have reported the genetic background related to the development of MPNST, which is usually a combination of the loss of function of *NF1* gene and genetic mutations, such as *TP53* and *CDKN2A* [5–7], the tumor microenvironment of MPNST, which is identified as one of the determinants of cancer malignancy, is less well-understood. The tumor microenvironment is composed of a wide variety of elements that include cellular elements, such as tumor-associated macrophages and cancer-associated fibroblasts, humoral factors in blood or those secreted from tumor cells, and hypoxic environment caused by insufficient blood flow due to tumor growth [8–11]. Moreover, although the effects of immune-related cells and humoral factors on tumor progression of MPNSTs have been investigated [12–14], there is insufficient literature on the present subject matter.

In this study, we analyzed the effect of adrenaline as a humoral factor that might affect the development of MPNST. Adrenaline is mainly secreted from the adrenal medulla into the bloodstream and circulates throughout the body. It is also synthesized by some

neurons in the central nervous system to serve as a neurotransmitter [15]. The effect of adrenaline on cancer progression has been reported in various cancer types in the terms of stress-triggered cancer progression [16–18]. Interestingly, adrenaline treatment at physiological concentrations (~nM) has been reported to advance breast cancer malignancy by increasing breast cancer cells stemness [19]. Cancer stem cells is a population of cells that is functionally defined by their ability to self-renew and maintain an undifferentiated state. They are considered as the cause of cancer tissue heterogeneity and resistance to treatment [20,21]. They have also been identified as a cell population with high expression levels of nerve growth factor receptors (NGFR, p75) and CD133 (Prominin 1) in MPNST [22,23]. If the adrenergic signals contribute to the progression of MPNST and if the molecular mechanism by which adrenaline regulates MPNST cancer stemness can be elucidated, it may be possible to establish a novel therapeutic approach against MPNST.

2. Materials and Methods

2.1. Cell culture and reagents

Human MPNST cell line FMS-1 was kindly provided by Dr. Hakozaki (Fukushima

Medical University) and HS-PSS was purchased from RIKEN BioResource Research Center (RCB2362). Cells are maintained in RPMI-1640 (FUJIFILM Wako Chemicals, Osaka, Japan) supplemented with 10% fetal bovine serum (FBS) (Corning, Glendale, AZ, USA) and antibiotics (FUJIFILM Wako Chemicals). For sphere formation assay, 1000 cells were seeded onto one well of ultra-low attachment 24-well plate (Corning) in 1.5 mL of Neurobasal medium (Thermo Fisher Scientific, Waltham, MA, USA) supplemented with B-27 and N-2 supplement (Thermo Fisher Scientific), 20 ng/mL of human epidermal growth factor (EGF), 20 ng/mL of human fibroblast growth factor-2 (bFGF) (FUJIFILM Wako Chemicals), 10 μg/mL of heparin (Sigma-Aldrich, St. Louis, MO, USA). Adrenaline and propranolol were purchased from TCI (Tokyo, Japan).

2.2. Lentivirus preparation and infection

For RNA interference experiments, we prepared shRNA-expressing lentivirus particles as previously described [24]. Briefly, we transfected 293FT cells (Thermo Fisher Scientific) with pLKO.1-puro-shRNA expressing vector, psPAX2, and pMD2.G (Addgene) using TransIT-LT1 Transfection Reagent (TaKaRa Bio, Shiga, Japan) and Opti-MEM (Thermo Fisher Scientific). The virus-containing medium was harvested after

60 hours of transfection. All sequences of shRNA are listed in Table S1.

2.3. Human tumor specimens

Human MPNST specimens, relevant information and anonymized medical data were obtained from Okayama University Hospital, following approval by the ethical committee of the hospital (approval number: 2009-032). All experiments with human specimens were carried out in accordance with the Declaration of Helsinki. Informed consent was obtained in the form of opt-out on the web-site of Okayama University Hospital (http://www.hsc.okayama-u.ac.jp/ethics/koukai/files/2009-032.pdf). Patients' information of sex, age, and ethnicity is described in Table S2.

2.4. Bioinformatics

Gene expression dataset was obtained from GEO public resource (http://www.ncbi.nlm.nih.gov/geo/) (accession number: GSE66743) [25]. The normalized values from the dataset were analyzed for Kaplan-Meier analysis and Gene Set Enrichment Analysis (GSEA, version 4.1.0). We divided the dataset into high and low categories based on mean expression value of the genes. ADRB2-correlated gene sets were obtained by running 1000 permutations of the gene set using a weighted

enrichment statistic. Gene sets were filtered for a minimum of 15 and a maximum of 500 genes and genes were ranked by signal to noise ratios for the curated gene sets (c2.all.v7.1.symbols.gmt and c5.all.v7.1.symbols.gmt). Gene sets with $P < 0.05$ and false-discovery rate (FDR) < 0.25 were considered to be significantly enriched.

2.5. Immunofluorescence staining and imaging

Fixed cells or deparaffinized sections were blocked with 3% bovine serum albumin (BSA) (Sigma-Aldrich) for 1 hour at room temperature, followed by overnight primary antibody incubation at 4°C and 1 hour secondary antibody incubation at room temperature. The stained samples were mounted with ProLong Diamond Antifade Mountant with DAPI (Thermo Fisher Scientific). Imaging was done using the confocal laser-scanning microscope LSM780 (Carl Zeiss, Oberkochen, Germany). The antibody information is described in Table S3.

2.6. RNA isolation and quantitative RT-PCR

Total RNA was isolated using TRIzol reagent (Thermo Fisher Scientific). After treatment with recombinant DNase I (TaKaRa Bio), the isolated RNAs were incubated with PrimeScriptTM RT Master Mix (TaKaRa Bio) to synthesize cDNA. Quantitative

real-time polymerase chain reaction (qRT-PCR) was performed using Luna Universal qPCR Master Mix (New England Biolabs, Ipswich, MA, USA) and Rotor-Gene 2plex HRM (Qiagen, Venlo, the Netherlands). All primer sequences are listed in Table S1.

2.7. Western blotting

Western blotting was performed as previously described [26]. Briefly, the cells were lysed with lysis buffer (20 mM Tris-HCl (pH = 7.5), 150 mM NaCl, 1 mM EDTA, 1 mM Na2EGTA, 0.5% Triton X-100) supplemented with complete protease inhibitor cocktail and PhosSTOP phosphatase inhibitor cocktail (Sigma-Aldrich). The samples were subjected to sodium dodecyl sulfate-polyacrylamide gel electrophoresis, transferred to polyvinylidene difluoride membrane (Sigma-Aldrich), and subjected to immunodetection. The signals were detected with Clarity Western Enhanced Chemiluminescence Substrate (Bio-Rad, Berkeley, CA, USA) and ChemiDoc imaging system (Bio-Rad). Details of the antibodies are described in Table S3.

2.8. Quantification and statistical analysis

Quantification of the immunostaining signals was done using ImageJ software (National Institutes of Health, Bethesda, Maryland, USA). Unpaired two-tailed t-test was

used to assess the differences between two groups. One-way ANOVA with Tukey's multiple comparisons post hoc test was used for the comparison of more than two groups. Log-rank test was used for survival analysis. $P < 0.05$ was considered statistically significant. The significance level was defined as ns (no significance), $*P < 0.05$; $**P < 0.01$; $***P < 0.001$; $****P < 0.0001$. All analyses were performed using GraphPad Prism version 8.0.0 for Windows (GraphPad Software, San Diego, California, USA)

3. Results

3.1. Adrenaline treatment expands the population of MPNST stem-like cells

To ascertain whether adrenaline treatment affects the stemness of MPNST cells, we first ascertained whether adrenaline treatment affected the self-renewal capacity of MPNST cells. Two MPNST cell lines (FMS-1 and HS-PSS) were subjected to this assay and we found that the number of spheres increased in an adrenaline concentration-dependent manner in both cell lines (Fig. 1A). Western blot analysis of these cells (cultured for 5 days in 2% FBS-medium containing 0, 1, 5, and 10 nM of adrenaline, respectively) showed that the expression levels of β-catenin (which is

important for the development of MPNST [27]), NGFR, and CD133 increased in an adrenaline concentration-dependent manner (Fig. 1B). Our finding on the upregulation of β-catenin expression by adrenaline treatment is consistent with the results of a previous study in breast cancer [19]. Immunostaining analysis showed that the number of cells expressing NGFR was significantly increased in cells treated with 10 nM adrenaline when compared to those treated with DMSO (as negative control) (Fig. 1C). These data indicate that adrenaline treatment enhances MPNST cells stemness.

3.2. ADRB2 is involved in the adrenaline-enhanced MPNST cells stemness

Adrenaline binds and activates adrenergic receptors, which consist of subfamilies of alpha-1A, -1B, and 1D; alpha-2A, -2B, and -2C; and beta-1, -2, and -3 [28]. To verify which adrenergic receptors are responsible for the stemness-promoting effects of adrenaline on MPNST, we profiled the expression levels of adrenergic receptors in MPNST cells. qRT-PCR analysis revealed that only three types of mRNA expression were confirmed in the cells: *ADRA1B*, *ADRA2B*, and *ADRB2* (which encodes alpha-1B, alpha-2B, and beta-2 adrenergic receptor, respectively) (Fig. S1A). Western blot analysis confirmed the protein expressions both in FMS-1 and HS-PSS cells (Fig. S1B).

We then analyzed how the expression level of each receptor affects the prognosis of MPNST patients. For this, we analyzed a public dataset of gene expression profiling, which included 30 MPNST patient samples (Kolberg cohort, deposited in GEO: GSE66743), and examined the relationship between the mRNA expression levels and prognosis. We found that, among the three adrenergic receptors, only *ADRB2* expression levels seem to determine the prognosis of the MPNST patients (Fig. 2A, Fig. S1C). In this dataset, the expression levels of *ADRB2* were positively correlated with those of *PROM1* (encoding CD133) (Fig. S1D). Immunostaining analysis revealed that NGFR and ADRB2 signals overlapped in cells treated with 10 nM adrenaline (Fig. 2B), thus indicating that protein levels of NGFR was elevated in $ADRB2^{High}$ cells. These data suggest that the beta-2 adrenergic receptor may be involved in maintaining the MPNST cells stemness.

To confirm that beta-2 adrenergic receptor contributes to the adrenaline-induced enhancement of MPNST cells stemness, we ascertained whether propranolol, an antagonist of beta-2 adrenergic receptor, inhibits the adrenaline effect on MPNST. Sphere formation assay showed that 10 μM propranolol treatment inhibited the

adrenaline-triggered increase of self-renewal capacity both in FMS-1 and HS-PSS cells (Fig. 2C). Western blot analysis confirmed that it could also inhibit the adrenaline-induced upregulation of β-catenin, NGFR, and CD133 (Fig. S1E). RNA interference experiments further revealed that the increase of self-renewal capacity upon adrenaline treatment was inhibited in ADRB2-knockdown cells (Fig. 2D). Western blot analysis of cell lysates from these cells showed that NGFR and CD133 were not upregulated by adrenaline stimulation in ADRB2-knockdown cells (Fig. 2E). These data indicate that the beta-2 adrenergic receptor is crucial for the adrenaline-driven enhancement of MPNST stemness.

3.3. Adrenaline enhances YAP/TAZ activity via ADRB2

To understand the molecular mechanism by which adrenaline enhanced the stemness of MPNST cells, we analyzed the patient dataset of GSE66743. Gene Set Enrichment Analysis (GSEA) in *ADRB2*^{High} and *ADRB2*^{Low} patient groups identified several gene sets related to stemness and YAP signaling pathway (Fig. 3A). Recently, the Hippo signaling transducer YAP and TAZ have been reported as a critical factor that promotes progression and malignant transformation of MPNST [29]. An increasing body of

evidence indicates that YAP/TAZ is a pivotal transcriptional regulator of stemness in many cancer types [30,31]. The activity of YAP/TAZ is regulated by the canonical Hippo kinases, mechanotransduction, and G protein-coupled receptor signaling [32] and it has been reported to cross-talk with a variety of signaling pathways, including WNT/β-catenin. [33]. Since adrenaline treatment enhanced MPNST cells stemness and increased the protein level of β-catenin (Fig. 1), we hypothesized that YAP/TAZ is involved in these phenomena. In fact, treatment of MPNST cells with adrenaline increased the protein expression of both YAP and TAZ as well as its target genes AXL and CYR61 (Fig. 3B, Fig. S2A). This effect was inhibited by propranolol treatment, thus suggesting that beta-2 adrenergic receptor-mediated signaling is required for activation of YAP/TAZ (Fig. 3B, Fig. S2A). Furthermore, immunostaining analysis revealed that adrenaline treatment significantly increased the activated (nuclear-localized) YAP and this effect was inhibited upon propranolol treatment (Fig.3C, Fig. S2B). RNA interference experiments confirmed that ADRB2 was essential for the enhancement of YAP/TAZ activity by adrenaline (Fig. 3D). These data indicate that adrenaline treatment activates the ADRB2-YAP/TAZ axis in MPNST cells, thereby resulting in enhanced stemness of the cells.

3.4. The ADRB2-YAP/TAZ axis defines the prognosis of MPNST patients

To verify that the ADRB2-YAP/TAZ axis contributes to the prognosis of MPNST, we performed immunostaining analysis in 15 patient specimens obtained from Okayama University Hospital (Fig. 4A). Confocal microscopy revealed that sections of primary tumors from patients who developed metastases showed significantly higher levels of both ADRB2 and YAP expression (Fig. 4B) and that both signals showed a positive correlation (Fig. 4C). Moreover, patients with high immunostaining signals of ADRB2 or YAP showed worse probability of survival than those with low staining signals (Fig.4D). These data indicate that the ADRB2-YAP/TAZ axis exacerbates the prognosis of MPNST patients.

4. Discussion

In this study, we demonstrated that adrenaline enhances MPNST cells stemness via ADRB2-YAP/TAZ axis. In MPNST cells, adrenaline treatment enhanced self-renewal capacity in a concentration-dependent manner and increased the expression of stem cell markers, such as NGFR and CD133 (Fig.1). The adrenaline-triggered enhancement of MPNST cells stemness depends on ADRB2-mediated signaling, as proven by results of

the antagonist treatment and ADRB2-knockdown experiments (Fig.2, Fig. S1). Since the effect of adrenaline on MPNST cells was not inhibited by the alpha-1/2 adrenergic receptor antagonist phentolamine (data not shown), it is clear that adrenaline indeed enhances MPNST cells stemness via ADRB2 receptor.

We further demonstrated that YAP/TAZ was activated during the adrenaline-induced stemness enhancement of MPNST cells (Fig.3, Fig. S2). Past studies reported that YAP/TAZ potentiated cancer stemness and worsened the disease prognosis in many types of cancer [30,31]. We observed that ADRB2 and YAP staining, whose signals were positively correlated, were significantly higher in metastatic cases and that the patient group with higher ADRB2 and YAP staining had a worse prognosis (Fig. 4).

According to a previous report, the blood adrenaline concentration in healthy individuals is approximately 0.1 nM [34]. In our data, enhanced self-renewal capacity and increased protein levels of stem cell markers and YAP/TAZ were observed with treatment with 1–10 nM adrenaline. On the other hand, a previous literature reported that higher concentration of adrenaline has an inhibitory effect on YAP/TAZ [35]. In that report, cells were treated with higher concentrations of adrenaline, maximum up to 10

μM (about 100,000 times higher than physiological concentrations). It is unclear whether the treatment could mimic the patho-physiological microenvironment in actual human cancer tissues. The fact that low concentrations of adrenaline activate YAP/TAZ and that high concentrations of adrenaline suppress YAP/TAZ suggest a difference in the downstream effects of adrenergic receptors on YAP/TAZ. Considering that ADRB2 is critical in the adrenaline-enhanced stemness of MPNST cells, our findings suggest that when physiological concentrations of adrenaline continue to act on cancer tissues with heterogeneity in adrenergic receptor expressions, YAP/TAZ continues to be activated in the cancer cells that express high levels of beta-2 adrenergic receptor, thereby resulting in the selected expansion of the cancer stem-like cell population in MPNST. Our data indicate that ADRB2 and its related signals may be good therapeutic targets in MPNST.

Funding: This work was supported by the Grant-in-Aid for Scientific Research from the Ministry of Education, Culture, Sports, Sciences, and Technology of Japan (grant number 20K07618) and the Japan Agency for Medical Research and Development (AMED) (grant numbers 18072932 and 20318557) and the Naito Foundation.

Declaration of Competing Interest

The authors declare no competing interests.

Acknowledgements

We thank ENAGO for English language processing and editing.

Supplementary data

Supplementary Figures (Fig. S1 and S2) and Supplementary Tables (Table S1 and S3) are found at XXX.

References

[1] S.L. Carroll. The challenge of cancer genomics in rare nervous system neoplasms: malignant peripheral nerve sheath tumors as a paradigm for cross-species comparative oncogenomics. Am J Pathol. 186 (2016) 464–477. https://doi.org/10.1016/j.ajpath.2015.10.023.

[2] J. Korfhage, D.B. Lombard. Malignant peripheral nerve sheath tumors: from epigenome to bedside. Mol Cancer Res. 17 (2019) 1417–1428. https://doi.org/ 10.1158/1541-7786.MCR-19-0147.

[3] K.M. Reilly, A. Kim, J. Blakely, et al. Neurofibromatosis Type 1-associated MPNST state of the science: outlining a research agenda for the future. J Natl Cancer Inst. 109 (2017) djx124. https://doi.org/ 10.1093/jnci/djx124.

[4] M. Kolberg, M. Holand, T.H. Agesen, et al. Survival meta-analyses for >1800 malignant peripheral nerve sheath tumor patients with and without neurofibromatosis type 1. Neuro Oncol. 15 (2013) 135–147. https://doi.org/ 10.1093/neuonc/nos287.

[5] A.S. Brohl, E. Kahen, S.J. Yoder, et al. The genomic landscape of malignant peripheral nerve sheath tumors: diverse drivers of Ras pathway activation. Sci Rep. 7 (2017) 14992. https://doi.org/ 10.1038/s41598-017-15183-1.

[6] R.M. Verdijk, M.A. den Bakker, H.J. Dubbink, et al. TP53 mutation analysis of malignant peripheral nerve sheath tumors. J Neuropathol Exp Neurol. 69 (2010) 16–26. https://doi.org/ 10.1097/NEN.0b013e3181c55d55.

[7] A. Pemov, H. Li, W. Presley, et al. Genetics of human malignant peripheral nerve sheath tumors. Neurooncol Adv. 2 (2019) i50–i61. https://doi.org/ 10.1093/noajnl/vdz049.

[8] A. Uneda, K. Kurozumi, A. Fujimura, et al. Differentiated glioblastoma cells accelerate tumor progression by shaping the tumor microenvironment via CCN1–mediated macrophage infiltration. Acta Neuropathol Commun. 9 (2021) 29. https://doi.org/ 10.1186/s40478-021-01124-7.

[9] H. Yoon, C.M. Tang, S. Banerjee, et al. Cancer-associated fibroblast secretion of PDGFC promotes gastrointestinal stromal tumor growth and metastasis. Oncogene. Feb 18. (2021) https://doi.org/ 10.1038/s41388-021-01685-w.

[10] A. Fujimura, H. Michiue, Y. Cheng, et al. Cyclin G2 promotes hypoxia–driven local invasion of glioblastoma by orchestrating cytoskeletal dynamics. Neoplasia. 15 (2013) 1272–1281. https://doi.org/ 10.1593/neo.131440.

[11] A.H. Kamdje, P.F. Etet, R.S. Tagne, L. Vecchio, K.E. Lukong, M. Krampera. Tumor microenvironment uses a reversible reprogramming of mesenchymal stromal

cells to mediate pro-tumorigenic effects. Front Cell Dev Biol. 8 (2020) 545126. https://doi.org/ 10.3389/fcell.2020.545126.

[12] J. Banerjee, R.J. Allaway, J.N. Taroni, et al. Integrative analysis identifies candidate tumor microenvironment and intracellular signaling pathways that define tumor heterogeneity in NF1. Genes. 11 (2020) 226. https://doi.org/ 10.3390/genes11020226.

[13] J.A. Stratton, P. Assinck, S. Sinha, et al. Factors within the endoneurial microenvironment act to suppress tumorigenesis of MPNST. Front Cell Neurosci. 12 (2018) 356. https://doi.org/ 10.3389/fncel.2018.00356.

[14] J.P. Brosseau, L.Q. Le. Heterozygous tumor suppressor microenvironment in cancer development. Trends Cancer. 5 (2019) 541–546. https://doi.org/ 10.1016/j.trecan.2019.07.004.

[15] A.W. Tank, D. Lee Won. Peripheral and central effects of circulating catecholamines. Compr Physiol. 5 (2015) 1–15. https://doi.org/ 10.1002/cphy.c140007.

[16] Y. Zhang, P. Zanos, I.L. Jackson, et al. Psychological stress enhances tumor growth and diminishes radiation response in preclinical model of lung cancer. Radiother Oncol. 146 (2020) 126–135. https://doi.org/ 10.1016/j.radonc.2020.02.004.

[17] X. Zhang, Y. Zhang, Z. He, et al. Chronic stress promotes gastric cancer progression and metastasis: an essential role for ADRB2. Cell Death Dis. 10 (2019) 788. https://doi.org/ 10.1038/s41419-019-2030-2.

[18] A. Iftikhar, M. Islam, S. Shepherd, et al. Cancer and stress: does it make a difference to the patient when these two challenges collide? Cancers (Basel). 13 (2021) 163. https://doi.org/ 10.3390/cancers13020163.

[19] B. Cui, Y. Luo, P. Tian, et al. Stress–induced epinephrine enhances lactate dehydrogenase A and promotes breast cancer stem–like cells. J Clin Invest. 129 (2019) 1030–1046. https://doi.org/ 10.1172/JCI121685.

[20] K.C. Genadry, S. Pietrobono, R. Rota, et al. Soft tissue sarcoma cancer stem cells: an overview. Front Oncol. 8 (2018) 475. https://doi.org/ 10.3389/fonc.2018.00475.

[21] Y. Arima, H. Nobusue, H. Saya. Targeting of cancer stem cells by differentiation therapy. Cancer Sci. 111 (2020) 2689–2695. https://doi.org/ 10.1111/cas.14504.

[22] M. Spyra, L. Kluwe, C. Hagel, R. et al. Cancer stem cell–like cells derived from malignant peripheral nerve sheath tumors. PLoS One. 6 (2011) e21099. https://doi.org/ 10.1371/journal.pone.0021099.

[23] A. Luscan, G. Shackleford, J. Masliah–Planchon, et al. The activation of the WNT signaling pathway is a Hallmark in neurofibromatosis type 1 tumorigenesis. Clin Cancer Res. 20 (2014) 358–371. https://doi.org/ 10.1158/1078-0432.CCR-13-0780.

[24] A. Fujimura, S. Yasui, K. Igawa, et al. In vitro studies to define the cell–surface and intracellular targets of polyarginine–conjugated sodium borocaptate as a potential delivery agent for boron neutron capture therapy. Cells. 9 (2020) 2149. https://doi.org/ 10.3390/cells9102149.

[25] M. Kolberg, M. Høland, G.E. Lind, et al. Protein expression of BIRC5, TK1, and TOP2A in malignant peripheral nerve sheath tumours--A prognostic test after surgical resection. Mol Oncol. 9(6) (2015) 1129-1139. https://doi.org/ 10.1016/j.molonc.2015.02.005.

[26] T. Yamamoto, A. Fujimura, F.Y. Wei, et al. 2–Methylthio Conversion of N6–isopentenyladenosine in mitochondrial tRNAs by CDK5RAP1 promotes the maintenance of glioma-initiating cells. iScience. 21 (2019) 42–56. https://doi.org/ 10.1016/j.isci.2019.10.012.

[27] A.L. Watson, E.P. Rahrmann, B.S. Moriarity, et al. Canonical Wnt/β–catenin signaling drives human Schwann cell transformation, progression, and tumor maintenance. Cancer Discov. 3 (2013) 674–689. https://doi.org/ 10.1158/2159-8290.CD-13-0081.

[28] M.J. Lohse, S. Engelhardt, T. Eschenhagen. What is the role of beta–adrenergic signaling in heart failure? Circ Res. 93 (2003) 896–906. https://doi.org/ 10.1161/01.RES.0000102042.83024.CA.

[29] L.M.N. Wu, Y. Deng, J. Wang, et al. Programming of Schwann Cells by Lats1/2–TAZ/YAP signaling drives malignant peripheral nerve sheath tumorigenesis. Cancer Cell. 33 (2018) 292–308. https://doi.org/ 10.1016/j.ccell.2018.01.005.

[30] M. Cordenonsi, F. Zanconato, L. Azzolin, et al The Hippo transducer TAZ confers cancer stem cell–related traits on breast cancer cells. Cell. 147 (2011) 759–772. https://doi.org/ 10.1016/j.cell.2011.09.048.

[31] F. Zanconato, M. Cordenonsi, Piccolo S. YAP and TAZ: a signalling hub of the tumour microenvironment. Nat Rev Cancer. 19 (2019) 454–464. https://doi.org/ 10.1038/s41568-019-0168-y.

[32] S. Piccolo, S. Dupont, M. Cordenonsi. The biology of YAP/TAZ: hippo signaling and beyond. Physiol Rev. 94 (2014)1287–1312. https://doi.org/ 10.1152/physrev.00005.2014.

[33] L. Azzolin, T. Panciera, S. Soligo, et al. YAP/TAZ incorporation in the β-catenin destruction complex orchestrates the Wnt response. Cell. 158 (2014) 157–170. https://doi.org/ 10.1016/j.cell.2014.06.013.

[34] C. Dodt, U. Breckling, I. Derad, et al. Plasma epinephrine and norepinephrine concentrations of healthy humans associated with nighttime sleep and morning arousal. Hypertension. 30 (1997) 71–76. https://doi.org/ 10.1161/01.hyp.30.1.71.

[35] F.X. Yu, B. Zhao, N. Panupinthu, et al. Regulation of the Hippo–YAP pathway by G-protein-coupled receptor signaling. Cell. 150 (2012) 780–791. https://doi.org/ 10.1016/j.cell.2012.06.037.

Figure 1. Adrenaline expands the population of MPNST stem-like cells.

(**A**) Adrenaline treatment potentiates the self-renewal capacity of FMS-1 and HS-PSS cells in a dose-dependent manner (n = 4, error bars indicate mean ± SD). (**B**) Adrenaline treatment elevated the expression levels of β-catenin, NGFR, and CD133 in a dose-dependent manner. The cells were grown in 2% FBS-containing culture medium with or without adrenaline for 5 days. (**C**) Immunofluorescent analysis showed that adrenaline treatment increased NGFR expression. Scale bars, 50 micrometer.

Figure 2. Beta-2 adrenergic receptor mediates the adrenaline-enhanced MPNST cells stemness.

(**A**) A Kaplan-Meir graph describing that higher expression levels of ADRB2 indicate a significantly worse prognosis of MPNST patients in the dataset of GSE66743 (*P* = 0.0203). (**B**) Immunostaining analysis using anti-NGFR and anti-ADRB2 antibodies showed that these two signals were overlapped in FMS-1 cells, indicating that ADRB2 was predominantly expressed in stem-like cells. Scale bars, 50 micrometer. (**C and D**) Propranolol (**C**) and ADRB2 knockdown (**D**) inhibited the adrenaline-induced enhancement of the self-renewal capacity of MPNST cell lines (n = 4, error bars indicate mean ± SD). (**E**) ADRB2 knockdown successfully attenuated the adrenaline-triggered expression of NGFR and CD133.

Figure 3. Adrenaline promotes the activity of YAP/TAZ via ADRB2

(**A**) GSEA indicates that the stem cell-related gene set and YAP-related gene set were enriched in the ADRB2High MPNST patients group in the dataset of GSE66743. (**B**) Adrenaline promotes the activity of YAP/TAZ in a dose-dependent manner. Propranolol successfully inhibits this activation. AXL and CYR61 served as YAP/TAZ target genes and GAPDH served as a loading control. (**C**) Immunofluorescent analysis showed that adrenaline treatment stimulates the nuclear accumulation of YAP, which was inhibited upon propranolol treatment. The graph indicates the percentage of the cells with nuclear YAP signal. Scale bars, 50 micrometer. (**D**) ADRB2 knockdown attenuated the adrenaline-driven activation of YAP/TAZ in MPNST cells.

Figure 4. The ADRB2-YAP/TAZ axis predicts the prognosis of MPNST patients.

(**A**) Immunofluorescent analysis of MPNST patients' specimens. Note that both ADRB2 and YAP signals were stronger the patients' specimen with metastasis (lower) than that without metastasis (upper). Scale bars, 50 micrometer. (**B**) Analysis of the quantified ADRB2 and YAP signals indicated that both ADRB2 and YAP signals were significantly elevated in the patients' specimen with metastasis. (**C**) The quantified signals of ADRB2 were positively correlated with those of YAP. (**D**) Higher signals of ADRB2 predict a significantly worse prognosis of MPNST patients (left, $P = 0.0113$). Although not statistically significant, higher signals of YAP also tend to indicate a worse prognosis of MPNST patients (right, $P = 0.08$).

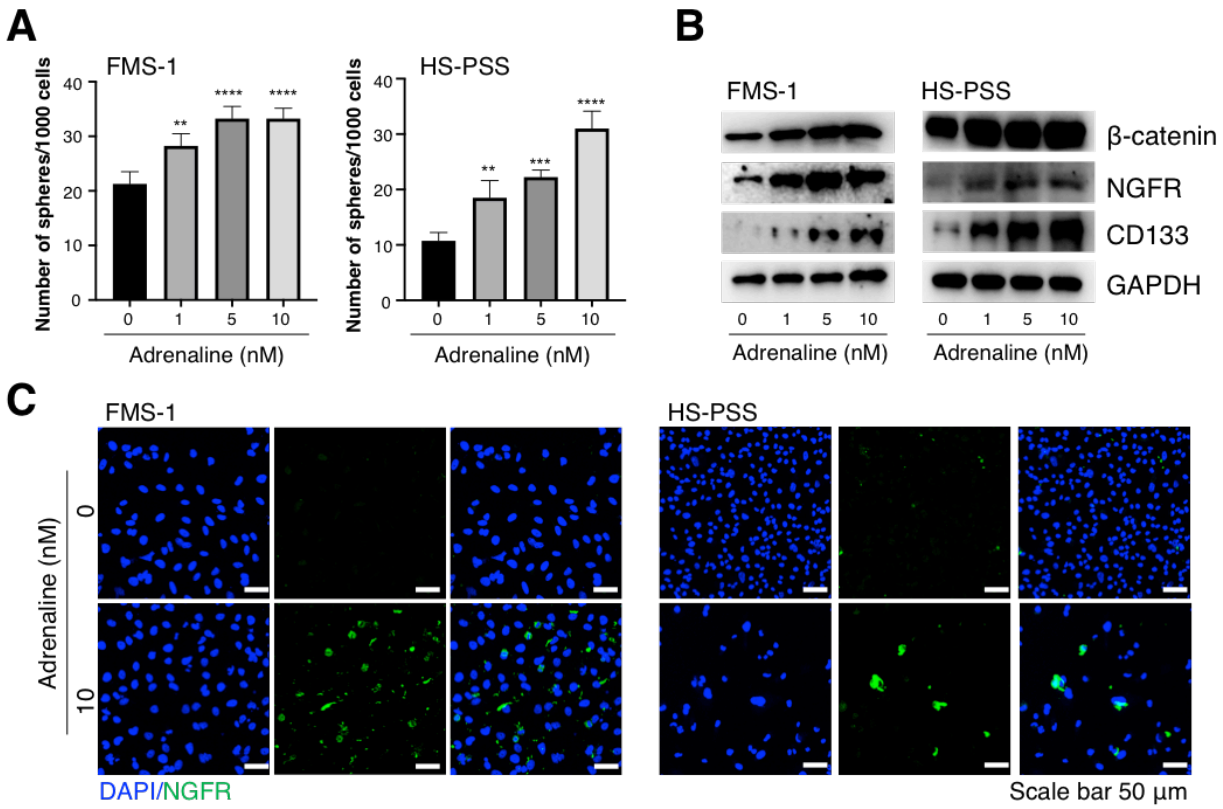

Figure 1 Huang/Fujimura et al.

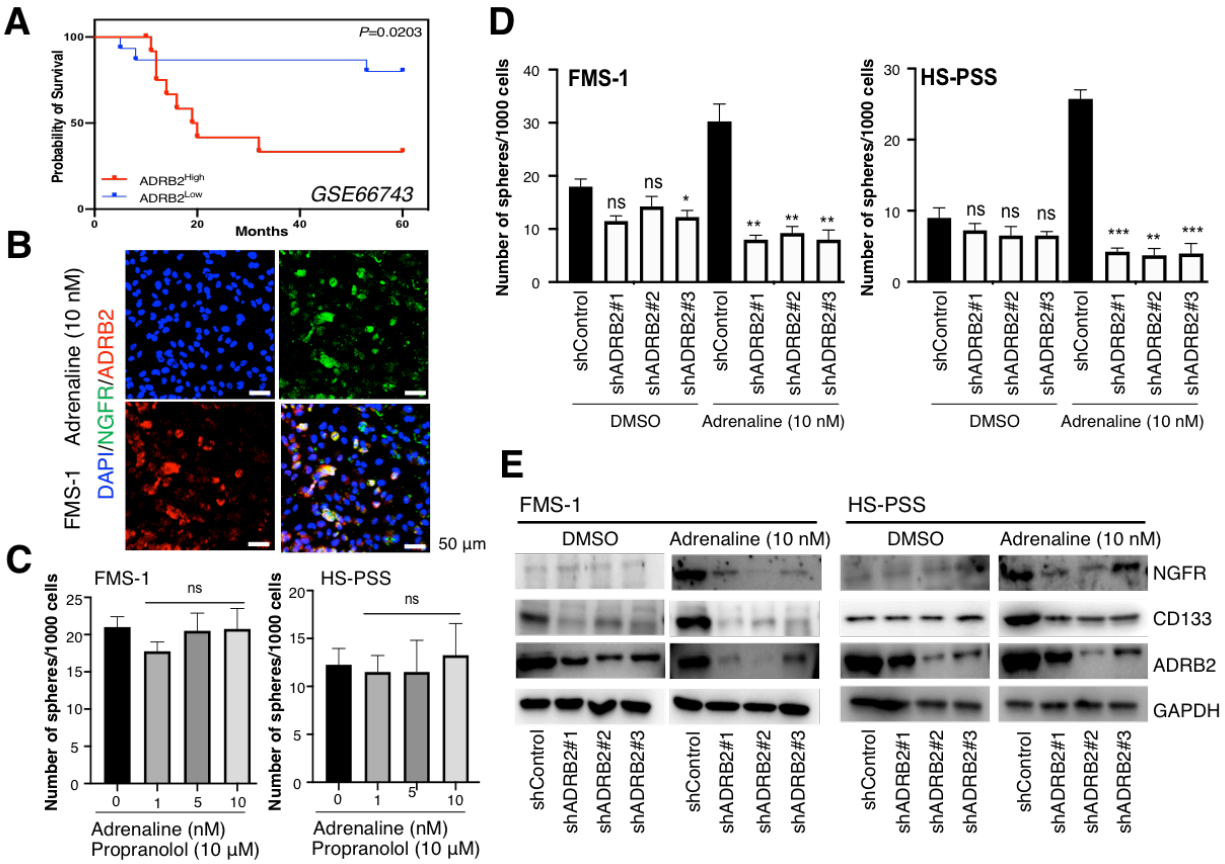

Figure 2 Huang/Fujimura et al.

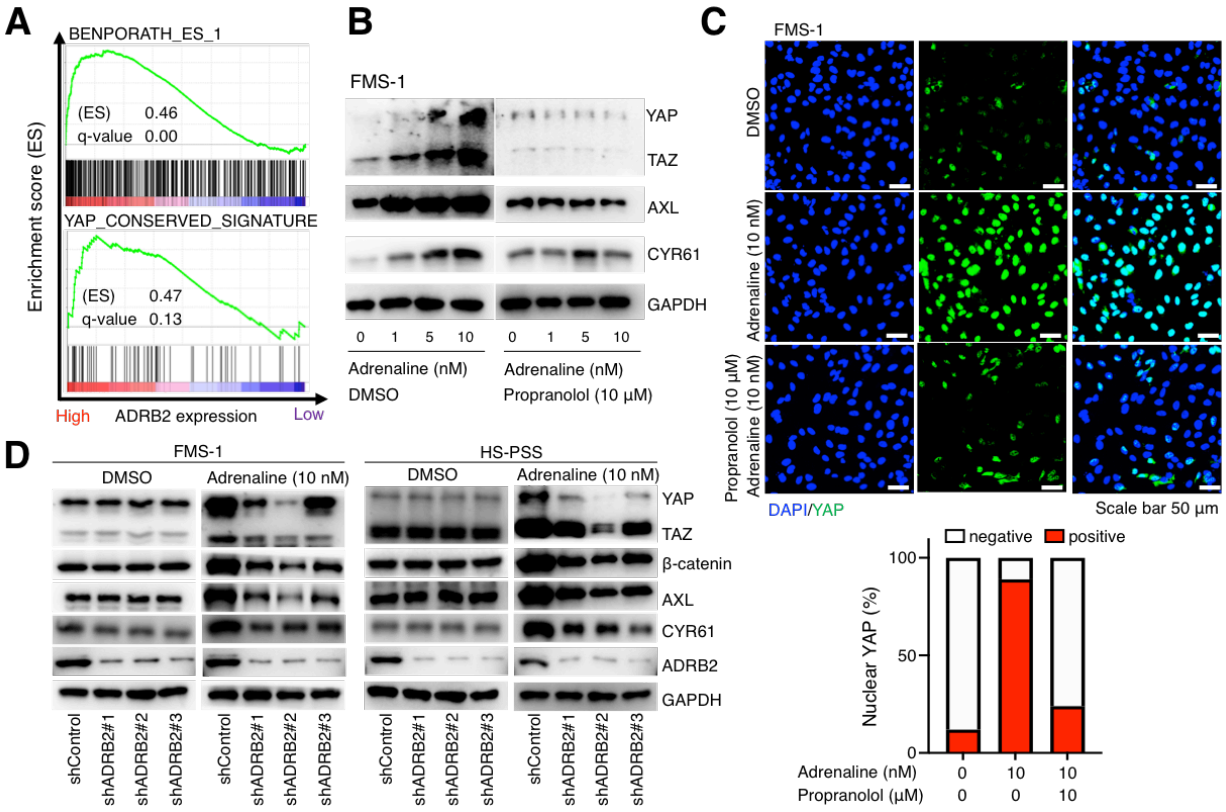

Figure 3 Huang/Fujimura et al.

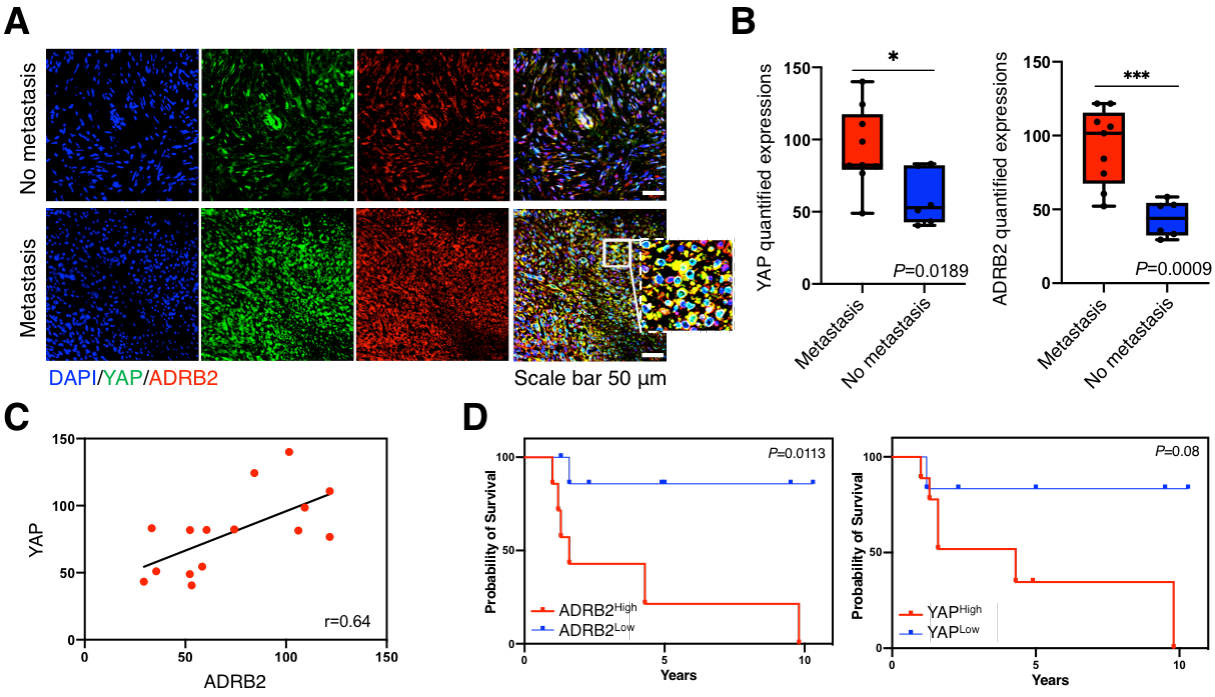

Figure 4 Huang/Fujimura et al.

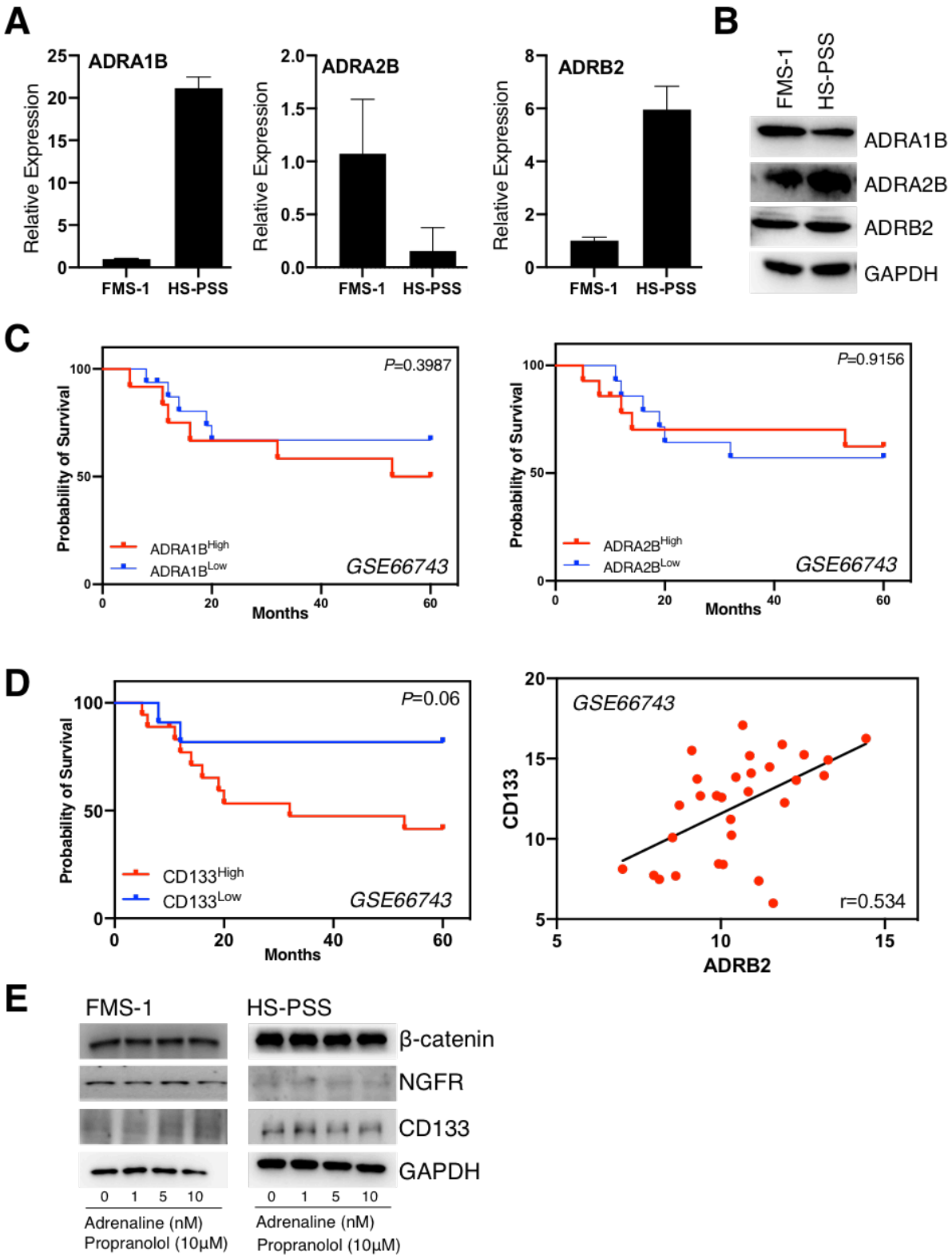

Figure S1 Huang/Fujimura et al.

Figure S1. Expression profiles of adrenergic receptors indicate that ADRB2 plays pivotal roles in the adrenaline-triggered enhancement of the stemness in MPNST cells, related to Figure 2.

(**A**) Quantitative PCR detected the expression of ADRA1B, ADRA2B, and ADRB2 in MPNST cell lines (n = 3, error bars indicate mean ± SD). (**B**) The protein expressions of ADRA1B, ADRA2B, and ADRB2 were confirmed by immunoblotting. (**C**) Kaplan-Meir graphs describing that there is no significant correlation between the expression levels of ADRA1B (left) and ADRA2B (right), and the prognosis of MPNST patients in the dataset of GSE66743. (**D**) Although it is not statistically significant, higher expression levels of PROM1 tend to indicate the worse prognosis of MPNST patients (P = 0.06). The expression levels of PROM1 are positively correlated with those of ADRB2. (**E**) Propranolol treatment inhibited the adrenaline-enhanced expression of β-catenin, NGFR, and CD133.

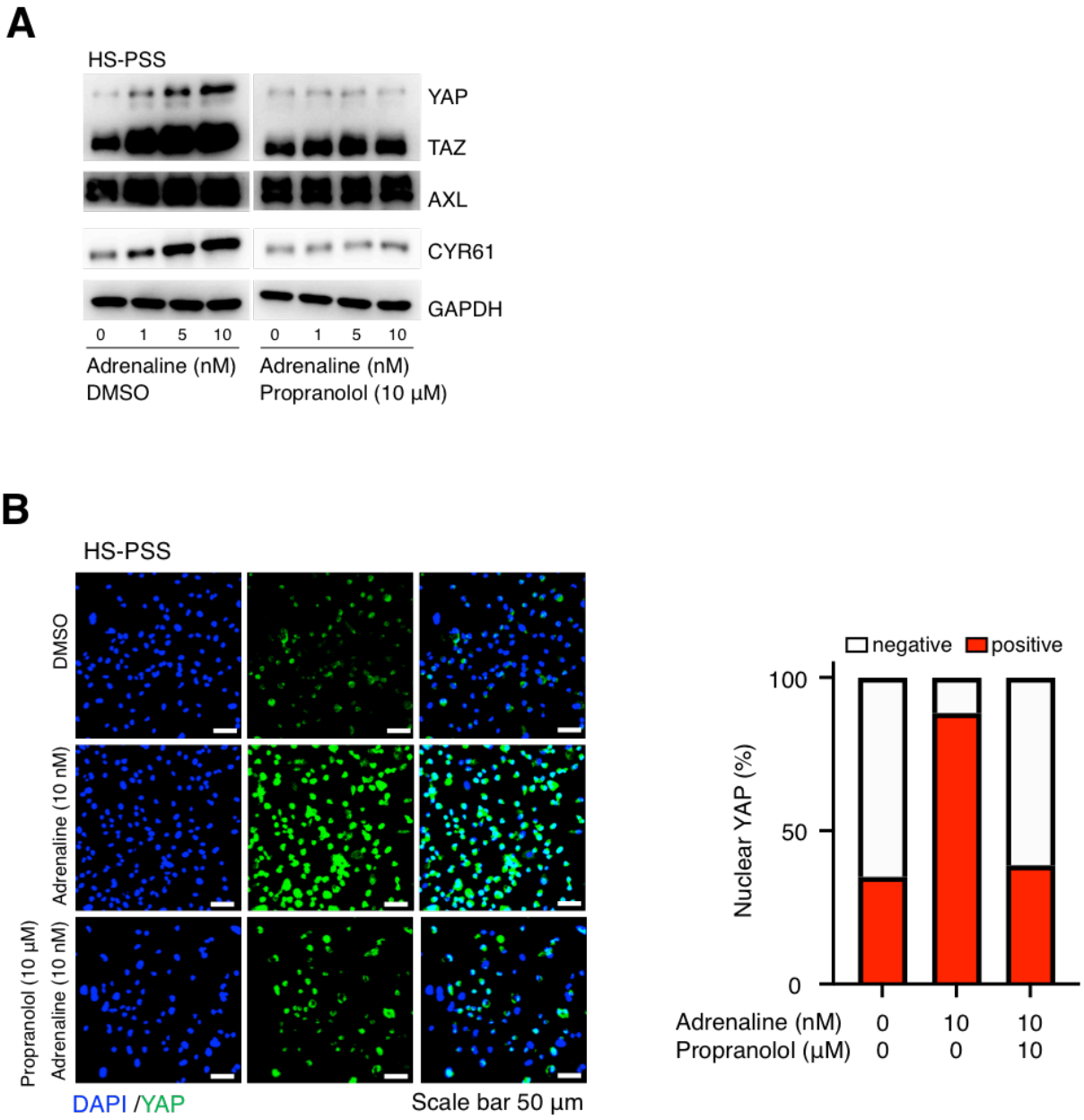

Figure S2 Huang/Fujimura et al.

Figure S2. Adrenaline enhances YAP/TAZ activity via ADRB2-dependent manner (related to Figure 3).

(**A**) Adrenaline promotes the activity of YAP/TAZ in a dose-dependent manner in HS-PSS cells. Propranolol successfully inhibited this activation. (**B**) Immunostaning showed that adrenaline treatment stimulates the nuclear accumulation of YAP in HS-PSS cells, which was inhibited upon propranolol treatment. The graph indicates the percentage of cells with nuclear YAP signal. Scale bars, 50 micrometer.

Primers for qPCR	**Sequences**
ADRA1A (Human) forward	CCAAGACGGATGGCGTTTG
ADRA1A (Human) reverse	TGGACACTGTAATCCTGGCAG
ADRA1B (Human) forward	CTTTCACGAGGACACCCTTAGC
ADRA1B (Human) reverse	GCCCAACGTCTTAGCTGCTT
ADRA1D (Human) forward	CTCCAGCCTGTCGCACAAG
ADRA1D (Human) reverse	TGTAGTCGGCCAATTCGTAGG
ADRA2A (Human) forward	AGAAGTGGTACGTCATCTCGT
ADRA2A (Human) reverse	CGCTTGGCGATCTGGTAGA
ADRA2B (Human) forward	GCTGTGGTCATTGGCGTTTTT
ADRA2B (Human) reverse	ACAGGGTTCAGTGAGCTGTTG
ADRA2C (Human) forward	GCCTCAACGACGAGACCTG
ADRA2C (Human) reverse	CCCAGCCCGTTTTCGGTAG
ADRB1 (Human) forward	ATCGAGACCCTGTGTGTCATT
ADRB1 (Human) reverse	GTAGAAGGAGACTACGGACGAG
ADRB2 (Human) forward	TGGTGTGGATTGTGTCAGGC
ADRB2 (Human) reverse	GGCTTGGTTCGTGAAGAAGTC
ADRB3 (Human) forward	GACCAACGTGTTCGTGACTTC
ADRB3 (Human) reverse	GCACAGGGTTTCGATGCTG
GAPDH (Human) forward	CTGGGCTACACTGAGCACC
GAPDH (Human) reverse	AAGTGGTCGTTGAGGGCAATG
shRNA	**Sequences**
shADRB2#1 (Human)	GGACCTGAGTCTGCTATATTT
shADRB2#2 (Human)	GAACACTAAACAGACTATTTA
shADRB2#3 (Human)	CCTCTTTGCATGGAATTTGTA

Table S1 Huang/Fujimura et al.

Specimen Number	Sex	Age	Ethnicity
1	Female	58	Asian
2	Male	30	Asian
3	Female	35	Asian
4	Female	64	Asian
5	Female	44	Asian
6	Male	35	Asian
7	Female	48	Asian
8	Female	36	Asian
9	Female	25	Asian
10	Female	22	Asian
11	Female	28	Asian
12	Male	28	Asian
13	Female	71	Asian
14	Male	55	Asian
15	Male	51	Asian

Table S2 Huang/Fujimura et al.

Antibodies	Source	Identifier (Cat No.)	Dilutions
Anti-GAPDH	Proteintech	60004-1-Ig	WB (1:2000)
Anti-CD133	Proteintech	18470-1-AP	WB (1:2000)
Anti-β-Catenin	BioLegend	862602	WB (1:2000)
Anti-NGFR	BioLegend	345102	WB (1:2000) IF (1:100)
Anti-ADRB2	Proteintech	13096-1-AP	WB (1:2000) IF (1:100)
Anti-ADRA1B	Proteintech	22419-1-AP	WB (1:2000)
Anti-ADRA2B	Proteintech	19778-1-AP	WB (1:2000)
Anti-YAP/TAZ	Santa Cruz Biotechnology	SC-101199	WB (1:1000) IF (1:50)
Anti-AXL	Proteintech	13196-1-AP	WB (1:2000)
Anti-CYR61	Cell Signaling Technology	39382	WB (1:2000)
Donkey anti-Rabbit IgG, Alexa Fluor Plus 594	Thermo Fisher Scientific	A32754	IF (1:200)
Donkey anti-Mouse IgG, Alexa Fluor 488	Thermo Fisher Scientific	A21202	IF (1:200)

Table S3 Huang/Fujimura et al.